coustics'08
Paris
June 29-July 4, 2008
www.acoustics08-paris.org

On effectiveness of vibration isolation using super-elastic rail support combined with booted sleeper or floating slab

Tianxing Wu

Shanghai Jiao Tong University, School of Mechanical Engineering, 800 Dong Chuan Road, 200240 Shanghai, China
txwu@sjtu.edu.cn

Ground-borne vibration or structure-borne vibration of viaduct due to railway traffic can be reduced by use of super-elastic rail support, booted-sleeper and floating-slab to isolate vibration transmission from the track to the infrastructure. In this study modeling of track structure dynamics and wheel/rail interaction is carried out in the frequency domain. Wheel/rail interaction and transmission to the infrastructure of the interaction force due to a relative displacement excitation are simulated. The effectiveness of vibration isolation is analyzed for the booted-sleeper or floating-slab track combined with super-elastic rail-fastener. It is found that the combined structure of booted-sleeper or floating-slab with super-elastic rail-fastener can effectively reduce the wheel/rail interaction force in the medium frequency region, compared with the booted-sleeper or floating-slab track using the usual rail-pad. The combination also shows better ability to block vibration transmission from the track to the infrastructure.

1 Introduction

Ground-bore vibration or structure-borne vibration and noise of viaduct caused by railway traffic is due to propagation of railway track vibration with the main components in the frequency range from tenths to hundreds Hertz [1, 2]. Measures to reduce the ground-borne or structure-borne vibration include super-elastic rail-fastener, booted-sleeper and floating slab track (FST) [3, 4].

The booted-sleeper track and FST reduce structure-borne vibration and noise via isolating vibration propagation from the track to the infrastructure. The super-elastic rail-fastener mitigates structure-borne vibration either through isolating vibration propagation to the infrastructure or through reducing the wheel/track dynamic interaction forces. This is because the rail support stiffness is effectively reduced by the super-elastic rail-fastener, as a result the wheel/track interaction forces due to the roughness on the wheel and rail treads are reduced. Although the slab support is soft for FST, the rail support stiffness may be high if stiff pads are used. Moreover, since the large inertia of the slab isolates the rail support from the slab bearings, the wheel/track interaction forces may be large due to the stiff pads.

Reduction of the wheel/track interaction force by use of super-elastic rail-fastener is beneficial to mitigate both structure-borne vibration and damage to the vehicle. Thus using the super-elastic rail-fastener combined with booted-sleeper or floating slab is expected to have better ability to control track vibration and noise than the usually used rail-pads. However, worries may arise: whether use of the super-elastic rail-fastener rather than the rail-pad, combined with the booted-sleeper or floating-slab, would degrade the performance on vibration isolation of the latter?

To answer the question, this study firstly develops a track model in the frequency domain and sets up a criterion of force transmission ratio to assess the effectiveness on vibration isolation for the booted-sleeper or floating-slab track combined with the super-elastic rail-fastener. Then a vehicle/track interaction model is developed and used to calculate the performance on vibration isolation under the circumstance of vehicle/track interaction for the track using the combined measures of vibration control.

2 Track model

To study the effectiveness on vibration isolation of a railway track, a calculation model is used as shown in Fig. 1. From the top to the bottom there are the rail, rail-pad, mass and elastic support layers [5]. As the track structure is symmetrical, only half a track is considered in the model. The rail is simplified to an infinite Euler beam. The rail-pad or super-elastic rail-fastener is simplified to a complex stiffness k_p. A mass layer with line density ρ_l represents the sleeper or floating slab. Another complex stiffness k_b represents the elastic support of the sleeper or slab. The rail-pad, mass and sleeper/slab bearing layers, i.e. k_p, ρ_l and k_b, are all supposed to be continuous. Such an assumption will bring convenience to simulation, and the errors caused can be ignored for analysis of track dynamics up to at least 600Hz. The continuously supported track model will give an average performance on vibration isolation for a FST and can not show the influences at higher frequencies of the slab modes. For short length slab below 2m, however, the errors can be ignored.

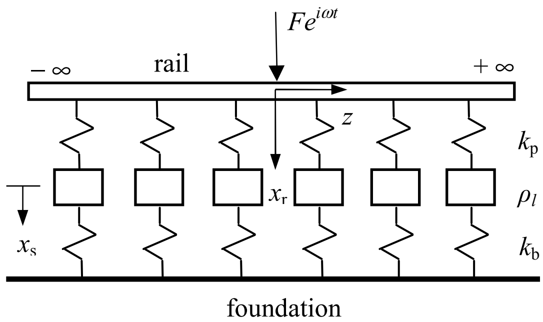

Fig. 1 Track model

In order to analyze the effectiveness on vibration isolation of the track structure, the wheel/track interaction is simplified to a harmonic excitation $Fe^{i\omega t}$ on the rail at z=0. In the simulations the effectiveness of the track can be assessed using the ratio of the transmitted force to the infrastructure to the excitation force on the rail, i.e. the force transmissibility. To calculate the transmitted force the track dynamic response must be known. The equations of motion for the rail and mass layer are given by

$$\rho_r A_r \frac{\partial^2 x_r}{\partial t^2} + E_r I_r \frac{\partial^4 x_r}{\partial z^4} + k_p (x_r - x_s) = F e^{i\omega t} \delta(z) \qquad (1)$$

$$\rho_l \frac{d^2 x_s}{dt^2} + (k_p + k_b) x_s - k_p x_r = 0 \qquad (2)$$

where ρ_r, A_r, x_r, E_r and I_r are the rail density, cross-sectional area, displacement, Young's modulus and area moment of inertia, respectively. ρ_l and x_s are the line density and displacement of the mass layer, respectively, that represents the sleeper or slab.

Assuming $x_r(z, t)=X_r(z)e^{i\omega t}$, $x_s(z, t)=X_s(z)e^{i\omega t}$ and substituting them in to Eqs. (1) and (2) results in

$$-\rho_r A_r \omega^2 X_r + E_r I_r X_r'''' + k_f X_r = F\delta(z) \tag{3}$$

where X_r and X_s are the displacement amplitude of the rail and mass layer respectively, ' stands for the derivative with respect to z, and k_f is the dynamic stiffness of the combined foundation under the rail, given as

$$k_f = \frac{k_p(k_b - \rho_l \omega^2)}{k_p + k_b - \rho_l \omega^2} \tag{4}$$

Rewriting Eq. (1) and treating the excitation as a boundary condition gives

$$E_r I_r X_r'''' + (k_f - \rho_r A_r \omega^2) X_r = 0 \tag{5}$$

$$\begin{cases} X_r'(0) = 0 \\ -E_r I_r X_r'''(0) = F/2 \end{cases} \tag{6}$$

The solution to Eq. (5) is

$$X_r = C_1 e^{k_1 z} + C_2 e^{k_2 z} + C_3 e^{k_3 z} + C_4 e^{k_4 z} \tag{7}$$

where $C_1 \sim C_4$ are constant, and $k_1 \sim k_4$ are the wavenumber, which are the roots of the following equation

$$k^4 = \frac{\rho_r A_r \omega^2 - k_f}{E_r I_r} \tag{8}$$

Wavenumber $k_1 \sim k_4$ consist of two pairs of conjugates, where those with negative real parts are for the wave propagating in the positive direction along the z axle, and those with negative real parts in the negative direction. Due to symmetry only the wave propagation in the positive direction is considered, thus the solution is given by

$$X_r = C_1 e^{k_1 z} + C_2 e^{k_2 z} \tag{9}$$

Through boundary condition, Eq. (6), C_1 and C_2 are worked out as

$$C_1 = -\frac{F/E_r I_r}{2k_1(k_2^2 - k_1^2)}, \quad C_2 = -\frac{F/E_r I_r}{2k_2(k_1^2 - k_2^2)} \tag{10}$$

The displacement of the mass layer can be determined using Eq. (2), given as

$$X_s = \frac{k_p}{k_p + k_b - \rho_l \omega^2} X_r \tag{11}$$

The force transmitted to the infrastructure is given by

$$F_b = \int_{-\infty}^{+\infty} k_b X_s(z) \mathrm{d}z \tag{12}$$

The force transmissibility to the infrastructure is defined by

$$T_F = |F_b|/F \tag{13}$$

and is used for assessing the performance on vibration isolation for the track structure.

3 Effectiveness on vibration isolation

In the calculations CHN60 (similar to UIC60) rail is used with cross-sectional area A_r=7.745×10^{-3}m^2 and area moment of inertia I_r=3.217×10^{-5}m^4. The parameters for the track are: k_p=100MN/m^2 and 20MN/m^2 for the rail-pad and super-elastic rail-fastener, respectively, ρ_l=300kg/m and 1000kg/m for the booted-sleeper and floating slab, k_b=25MN/m^2 and 15MN/m^2 for the support of the booted-sleeper and floating slab. k_p and k_b are complex stiffness with loss factor η =0.25. Using the above parameters, the natural frequency is 46Hz and 19.5Hz, respectively, for the booted-sleeper and floating-slab system.

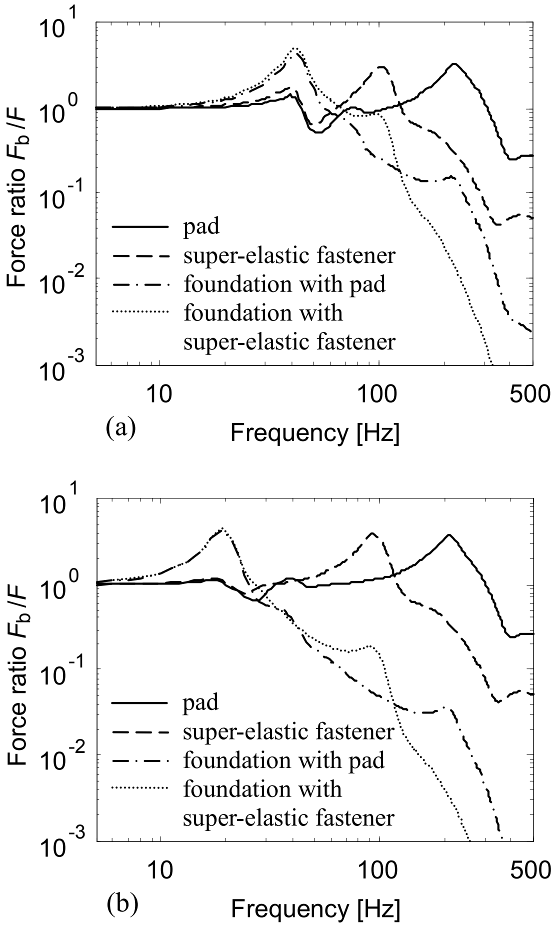

Fig. 2 Force transmissibility to rail support and infrastructure, (a) for booted-sleeper track, (b) for FST.

The calculation results are presented in terms of the force transmissibility to the rail-fastener and infrastructure. The force transmissibility to the infrastructure can be used to evaluate the effectiveness on vibration isolation of the track. The results shown in Fig. 2(a) are from the booted-sleeper track and in Fig. 2(b) from the FST. It can be seen that the force transmitted to the pad or super-elastic rail-fastener is almost not influenced by the base support type, i.e. the booted-sleeper or floating slab. For the rail-pad, whose stiffness is five times stiffer than the super-elastic rail-fastener, the highest force transmissibility appears at about 200Hz, whereas for the super-elastic rail-fastener the highest transmissibility appears at about 100Hz.

The force transmissibility to the infrastructure is close to one at low frequencies and greater than one around the first order natural frequency of the track, which is 46Hz and 19.5Hz for the booted-sleeper and floating-slab track respectively. Above √2 times the natural frequency, the force transmissibility becomes less than one and the track has the ability to isolate vibration.

From Fig.2 the force transmissibility to the infrastructure can be seen to have peaks corresponding to the frequencies, at which the force transmissibility to the pad or super-elastic rail-fastener shows peaks. The peak appears at about 100Hz for the track using the super-elastic rail-fastener and 200Hz for that using the rail-pad.

The force transmitted to the infrastructure caused by the harmonic excitation $Fe^{i\omega t}$ decays along the track. Fig. 3 shows the force transmission ratio to the foundation in one meter for the track with the booted-sleeper at z = 0, 1, 2, 4m, calculated by $T_F(z) = |k_b X_s(z)|/F$.

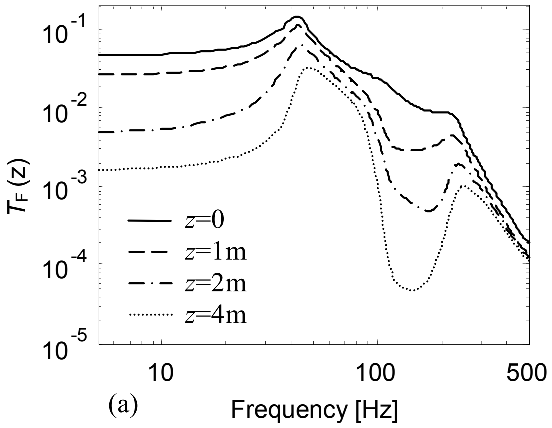

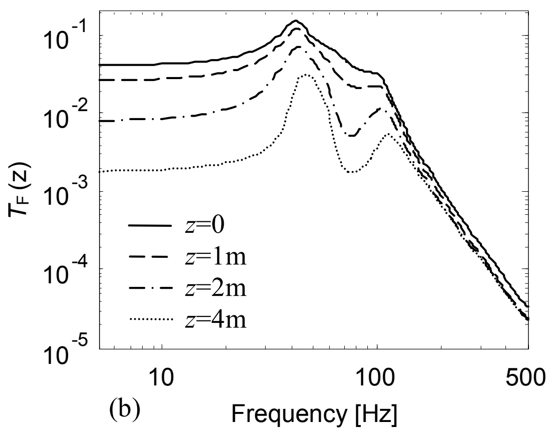

Fig. 3 Force transmissibility to infrastructure in unite length at different positions for booted-sleeper track, (a) using rail-pad, k_p=100MN/m^2, (b) using super-elastic rail-fastener, k_p=20MN/m^2.

The force to the infrastructure can be seen to decay similarly at low frequencies up to 50Hz for both using the rail-pad and using the super-elastic rail-fastener. At high frequencies above 250Hz the force transmission ratio is lower for the latter than for the former. In the medium frequency region the force ratio and the decay pattern are complicated. In the frequency range 100-220Hz the transmitted force decays very quickly for the track using the rail-pad, whereas for that using the super-elastic rail-fastener it days not quickly in the corresponding frequency range 60-100Hz. The force decay in the floating slab track is similar and thus not shown here.

4 Effectiveness under vehicle/track interaction

It is more practical that the effectiveness on vibration isolation of a track is assessed under the circumstance of vehicle/track interaction, as the wheel/rail interaction is effectively influenced by the track dynamics, and use of the super-elastic rail-fastener, booted-sleeper or floating slab will alter the dynamic behavior of the track.

When a vehicle runs over the rail, wheel/rail interaction happens due to the roughness on the wheel and rail contact surface, and causes the dynamic force between the wheel and rail. A wheel/track interaction model is depictured in Fig. 4, where the roughness on the wheel and rail treads is combined to form a relative displacement excitation [6]. The wheel is assumed to be stationary, whereas the relative displacement moves at vehicle speed v between the wheel and rail. As the vibration wave propagating speed in the rail is much higher than the train speed, such assumption of stationary wheel is reasonable and will not cause errors [7].

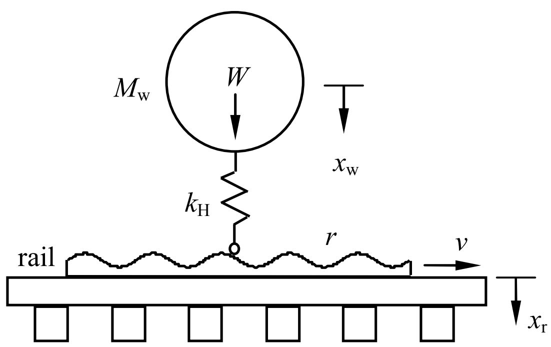

Fig. 4 Modelling of relative displacement excitation between the wheel and rail

In Fig.4 the wheel is simplified to a mass M_w, the contact stiffness is linearized and represented by stiffness k_H. The equation of motion for the mass wheel is given as

$$M_w \ddot{x}_w = -k_H (x_w - x_r + r) \tag{14}$$

where x_w is the wheel displacement, x_r is the rail displacement at the wheel/rail contact point, and r is the roughness excitation. The sign convention adopted here for downward x_w and x_r is positive, and for r is negative for a dip, positive for an asperity. As the natural frequency of the vehicle suspension system is much lower than that of the wheel/track vibration considered, the vehicle above the primary suspension is simplified to a static load W acting on the wheel. The static load W and the displacement caused by W can be counteracted each other and disappear in the equation of motion by properly choosing the origin of the coordinates.

According to Eq. (14) the force acting onto the rail can be calculated in the frequency domain by

$$F = k_H (X_w - X_r + R) \tag{15}$$

If the receptance of the wheel and track is known as α^w and α^r, respectively, which is defined as the displacement at the forcing point caused by a unite harmonic excitation, Eq. (15) can be written as

$$F = \frac{1}{\alpha^C}(-\alpha^w F - \alpha^r F + R) \tag{16}$$

where α^c=1/k_H is the receptance of the contact spring, and R is the combined wheel and rail roughness spectrum. From Eq. (16) the wheel/rail dynamic interaction force due to the roughness excitation can be determined by

$$F = \frac{R}{\alpha^w + \alpha^c + \alpha^r} \tag{17}$$

The receptance of the track can be calculated using the track model in Fig.1. A vehicle model composed of a single wheel and primary suspension, representing an eighth of a vehicle, is used to interact with the track. The following parameters are chosen in the calculations: the linearized contact stiffness k_H=1140MN/m, the wheel mass (unsprung mass) M_w=700kg. The bogie mass is 800kg, the stiffness is 9.35×10^5N/m for the primary suspension and the damping coefficient is 2.5×10^5Ns/m.

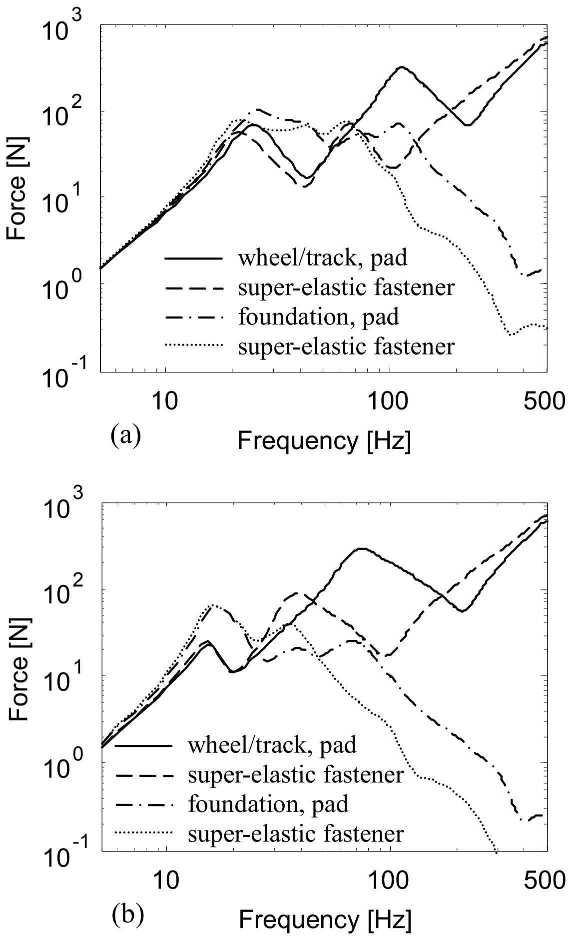

Fig. 5 Wheel/track interaction force and transmitted force to infrastructure due to 1μm roughness excitation: — wheel/track using rail-pad, – – wheel/track using super-elastic rail-fastener, – · – infrastructure with rail-pad, ···· infrastructure with super-elastic rail-fastener, (a) for booted-sleeper track, (b) for FST.

The wheel/track interaction force due to 1μm relative displacement excitation is calculated using Eq. (17), and the force transmitted to the infrastructure is calculated using Eq. (12). The results are shown in Fig. 5(a) and 5(b) for the booted-sleeper track and FST respectively. It can be seen that the wheel/track interaction forces are magnificently reduced in the medium frequency region when using the super-elastic rail-fastener. For the booted-sleeper track the frequency region is about 80-180Hz, and for the FST it is about 50-160Hz. As a result the forces transmitted to the infrastructure are also largely reduced, starting from 80Hz for the booted-sleeper track and 50Hz for the FST. This is beneficial both to control of the track vibration and reduction of the dynamic load onto the vehicle, although at certain frequencies in the low frequency region the forces transmitted to the infrastructure could become a bit larger compared with the tracks using the rail-pad. Nevertheless, use of the super-elastic rail-fastener combined with the booted-sleeper track or FST can effectively isolate the dynamic force transmission from the track to the infrastructure, and meanwhile, magnificently reduce the wheel/track interaction force in the medium frequency region.

5 Conclusion

A track model in the frequency domain is developed for the booted-sleeper and floating-slab track and a simplified vehicle model is introduced to interact with the track, in order to investigate the effectiveness on vibration isolation of the booted-sleeper or floating-slab track combined with the super-elastic rail-fastener. The force transmissibility to the infrastructure is used to assess the effectiveness on vibration isolation. The results show that above √2 times the natural frequency of the booted-sleeper or floating-slab the force transmissibility becomes less than one and the track has the ability to isolate vibration. Compared with the rail-pad, use of the super-elastic rail-fastener combined with either the booted-sleeper track or the FST can magnificently reduce the wheel/track interaction force in the medium frequency region, and thus shows better performance on vibration isolation. Reducing the wheel/track interaction force is also beneficial to reduction of the dynamic load onto the vehicle.

Acknowledgments

This study has been supported by the Opening Research Foundation of State Key Laboratory of Traction Power, under the project ‘Mechanism and Control of the Structure-born Noise from Viaduct of Railway Transportation’, Grant No. TPL0801.

References

[1] H. E. M. Hunt, "Modelling of rail vehicles and track for calculation of ground-vibration transmission into buildings", *Journal of Sound and Vibration* 193, 185-194 (1996)

[2] K. W. Ngai, C. F. Ng, "Structure-borne noise and vibration of concrete box structure and rail viaduct", *Journal of Sound and Vibration* 255, 281-297 (2002)

[3] J. T. Nelson, "Recent development in ground-borne noise and vibration control", *Journal of Sound and Vibration* 193, 367-376 (1996)

[4] B. Hemsworth, "Reducing groundborne vibrations: state-of-the-art study", *Journal of Sound and Vibration* 231, 703-709 (2000)

[5] D. J. Thompson, N. Vincent, "Track dynamic behaviour at high frequencies. Part 1: Theoretical models and laboratory measurements", *Vehicle System Dynamics* S24, 86-99 (1995)

[6] D. J. Thompson, "Wheel-rail noise generation, Part I: introduction and interaction model", *Journal of Sound and Vibration* 163, 387-400 (1993)

[7] T. X. Wu, D. J. Thompson, "On the parametric excitation of the wheel/track system", *Journal of Sound and Vibration* 278, 722-747 (2004)